Journal of Physics: Conference Series

Effect of Ni and Al substitution on the magnetic properties of Y-type hexaferrite $Ba_{0.5}Sr_{1.5}Zn_{0.5}Ni_{1.5}Fe_{11.92}Al_{0.08}O_{22}$ powders

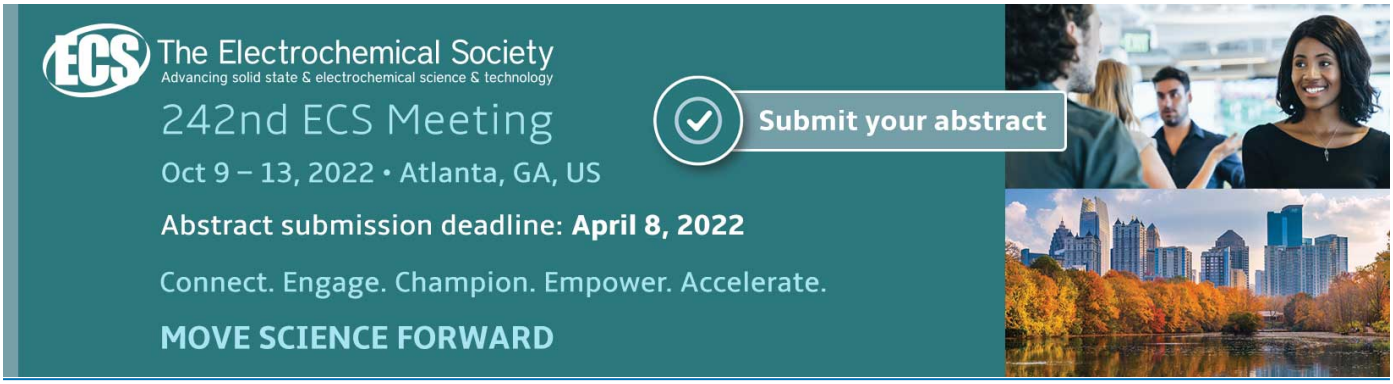

Journal of Physics: Conference Series **1859** (2021) 012067 doi:10.1088/1742-6596/1859/1/012067

Effect of Ni and Al substitution on the magnetic properties of Y-type hexaferrite $Ba_{0.5}Sr_{1.5}Zn_{0.5}Ni_{1.5}Fe_{11.92}Al_{0.08}O_{22}$ powders

B Georgieva[1], S Kolev[1,2], K Krezhov[1], Ch Ghelev[1], D Kovacheva[3], L-M Tran[4], M Babij[4], A Zaleski[4], B Vertruyen[5], R Closset[5] and T Koutzarova[1]

[1] Institute of Electronics, Bulgarian Academy of Sciences, 72 Tsarigradsko Chaussee, 1784 Sofia, Bulgaria
[2] Neofit Rilski South-Western University, 66 Ivan Mihailov Str., 2700 Blagoevgrad, Bulgaria
[3] Institute of General and Inorganic Chemistry, Bulgarian Academy of Sciences, Acad. Georgi Bonchev Str., bld. 11, 1113 Sofia, Bulgaria
[4] Institute of Low Temperature and Structure Research, Polish Academy of Sciences, ul. Okólna 2, 50-422 Wroclaw, Poland
[5] Greenmat, Chemistry Department, University of Liege, 11 allée du 6 août, 4000 Liège, Belgium

E-mail: b.georgiewa@abv.bg

Abstract. The effect is reported of substituting the non-magnetic Zn^{2+} cations with magnetic Ni^{2+} cations, and of the magnetic Fe^{3+} cations with non-magnetic Al^{3+} cations in $Ba_{0.5}Sr_{1.5}Zn_{0.5}Ni_{1.5}Fe_{11.92}Al_{0.08}O_{22}$ on the resulting magnetic properties. The Y-type hexaferrite powders were synthesized by citric acid sol-gel auto-combustion, followed by appropriate thermal annealing. The saturation magnetization values (M_s) in a magnetic field of 50 kOe were 36 emu/g and 30 emu/g at 4.2 K and 300 K, respectively. The zero-field-cooled (ZFC) and field-cooled (FC) magnetization vs. temperature (4.2 – 300 K) were measured in dc magnetic fields of 50 Oe, 100 Oe and 500 Oe. The changes resulting from the dissimilar cationic substitutions were identified and discussed.

1. Introduction

The multiferroic materials, which exhibit a simultaneous existence of long-range magnetic and ferroelectric orders, have recently driven significant research interest in the fields of both basic and applied sciences in search of promising materials for development of novel devices and technologies. In particular, the Y-type hexaferrites – $A_2Me_2Fe_{12}O_{22}$, where A = Ba, Sr and Me is a divalent cation, have been the subject of intensive characterization related to studying the magnetoelectric (ME) effect. $Ba_{0.5}Sr_{1.5}Zn_2Fe_{12}O_{22}$ is among the most promising Y-type hexaferrites exhibiting ME effect at room temperature. The crystal structure of Y hexaferrites belongs to the rhombohedral space group R(-3m). The unit cell contains three formula units (Z=3). The structure can be considered as consisting of two types of crystal S- and T-blocks consecutively stacked along the hexagonal *c* axis in the sequence (TST′ST″S″), with the primes indicating rotation about the *c*-axis by 120 degrees [1]. The hexagonal unit cell is thus made up of three T blocks and three S blocks, containing 18 oxygen layers. There are repeatedly four cubic close packed oxygen layers followed by two barium-containing hexagonal close-

packed layers, forming a close packing sequence. The S-block ($Me_2Fe_4O_8$; spinel block) can be thought of as a double spinel layer. There are six sites for metals, four of them octahedral and two tetrahedral. The T-block ($Ba_2Fe_8O_{14}$) is made up of four oxygen layers, with a barium atom substituting an oxygen atom in the inner two layers, which are opposite one another in the neighboring layers, resulting in two tetrahedral and six octahedral sites [1]. All cations (Me^{+2} and Fe^{+3}) are positioned in six specific crystallographic sites: two tetrahedral sites (6_{cIV} and 6_{c*IV}) and four octahedral sites (3_{aVI}, 3_{bVI}, 6_{cVI}, and 18_{hVI}). The Zn^{2+} cations prefer to occupy tetrahedral sites, together with the Fe^{3+} cations [2, 3]. The easy magnetization axis lies in a plane perpendicular to the *c*-axis direction, while the non-compensated magnetic moment lying in the *ab* plane arises from dominating majority spins in octahedral 3*a*, 3*b*, and 18*h* sites, and minority spins in tetrahedral $6c_T$ and $6c_S$ and octahedral 6*c* sites [4]. These majority and minority spins determine two magnetic sublattices that are different from the crystal structural blocks, namely, L_m (spins in octahedral 3_a, 3_b, and 18_h sites) and S_m (spins in tetrahedral 6_{cT} and 6_{cS} and octahedral 6_c sites) blocks alternating along [001], which bear, correspondingly, opposite large and small magnetization [5]. Taking into consideration these two sublattices, L_m and S_m, helps one understand the magnetic structures of Y-type hexaferrites because the strongest magnetic interaction occurs inside the T block. The super exchange interaction across the boundary of the sublattices, Fe(4)-O(2)-Fe(5), can be affected by a proper substitution, e.g. replacing large Ba^{2+} with smaller Sr^{2+} and the Y-type hexaferrite $Ba_{0.5}Sr_{1.5}Zn_2Fe_{12}O_{22}$ was the first hexaferrite, where ferroelectric polarization was found in a magnetic field-induced metamagnetic phase. Therefore, the T block, which contains the Fe(4)-O(2)-Fe(5) bonds, is essential to bring into being the non-collinear screw structure in the Y-type hexaferrite. It was shown that a small amount of Fe^{3+} substitutions by Al^{3+} lead to observation of ME room temperature effect at a low magnetic field [6]. As the ME effect is connected with the magnetic spin ordering, it is very important to study the influence of cation substitution on the magnetic phase transition temperatures. In our earlier works [7, 8] we showed that the partial substitution of Zn^{2+} by magnetic Ni^{2+} cations can increase the magnetic phase transition temperature.

Here we report studies on the effect of substituting the non-magnetic Zn^{2+} cations with magnetic cations Ni^{2+}, and of the magnetic Fe^{3+} cations with non-magnetic Al^{3+} cations in Y-type hexaferrite $Ba_{0.5}Sr_{1.5}Zn_2Fe_{12}O_{22}$ powders on their magnetic properties and magnetic-phase transitions.

2. Experimental

The $Ba_{0.5}Sr_{1.5}Zn_{0.5}Ni_{1.5}Fe_{11.92}Al_{0.08}O_{22}$ polycrystalline material was synthesized by citric acid sol-gel auto-combustion. The corresponding metal nitrates were used as starting materials, and a citric acid solution was slowly added to the mixed nitrates as a chelator to form stable complexes with the metal cations. The solution was slowly evaporated to form a gel, which was dehydrated at 120 °C, turned into a fluffy mass and burned in a self-propagating combustion manner. The auto-combusted material was annealed at 1170 °C in air.

The XRD measurements were carried out using a Brucker D8 Advanced diffractometer (40 kV, 30 mA) controlled by a DIFFRACT^{plus} software in Bragg-Brentano reflection geometry with Cu-Kα radiation (λ = 1.5418 Å). The magnetic properties were measured by means of a commercial physical-property-measurement-system (PPMS) from Quantum Design equipped with an ACMS option. The hysteresis measurements were conducted at 4.2 K and 300 K. The zero-field-cooled (ZFC) and field-cooled (FC) magnetization vs. temperature (4.2 – 300 K) measurements were performed at magnetic fields of 50 Oe, 100 Oe and 500 Oe. In the ZFC protocol, the sample under study was cooled from room temperature down to 4.2 K without any magnetic field; the magnetization was measured with the temperature being raised from 4.2 K to 300 K at a heating rate of 3 K/min in the applied magnetic field. The FC curve was recorded on the same sample upon cooling from 300 K to 4.2 K in the same magnetic field.

Results and discussion

The $Ba_{0.5}Sr_{1.5}Zn_{0.5}Ni_{1.5}Fe_{11.92}Al_{0.08}O_{22}$ was obtained as a well-crystallized polycrystalline powder. The room temperature XRD pattern of the final powder material reveals the formation of a well-defined hexagonal phase (figure 1).

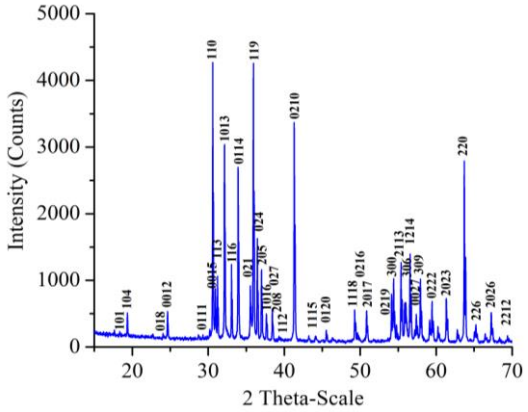

Figure 1. XRD patterns of $Ba_{0.5}Sr_{1.5}Zn_{0.5}Ni_{1.5}Fe_{11.92}Al_{0.08}O_{22}$ powder.

The very sharp and narrow peaks indicate a high degree of crystallinity and show the characteristic peaks (standard card ICSD-01-079-1409) corresponding to the Y-type hexaferrite structure.

Figure 2 presents the initial magnetization and the hysteresis loops of the powder material at 4.2 K and 300 K. At high magnetic fields, the magnetization almost reaches saturation. The values of M_s in a magnetic field H of 50 kOe were 36 emu/g and 30 emu/g at 4.2 K and 300 K, respectively. These values are lower than those of the polycrystalline $Ba_{0.5}Sr_{1.5}Zn_2Fe_{11.92}Al_{0.08}O_{22}$ material. This should be related to the known preference of the non-magnetic Zn^{2+} cations to occupy tetrahedral positions, whereas the magnetic Ni^{2+} cations prefer to enter octahedral positions [8]. This entails the migration of iron cations between crystallographic sites with octahedral and tetrahedral oxygen configuration and is accompanied by a corresponding change in the magnetic structure. The magnetization loop exhibits a small hysteresis at 4.2 K typical of a conical spin order phase; the coercive field H_c is 30 Oe. In the range –50 Oe to +50 Oe at 300 K the hysteresis curves behave like superparamagnetic ones – the remanence magnetization and coercive field values are zero. However, at a sufficiently higher magnetic field, the hysteresis effect becomes clear in the course of the magnetization. Similar behavior was observed for the first time in the hexaferrite $Ba_{0.5}Sr_{1.5}Zn_2Fe_{12}O_{22}$. [9].

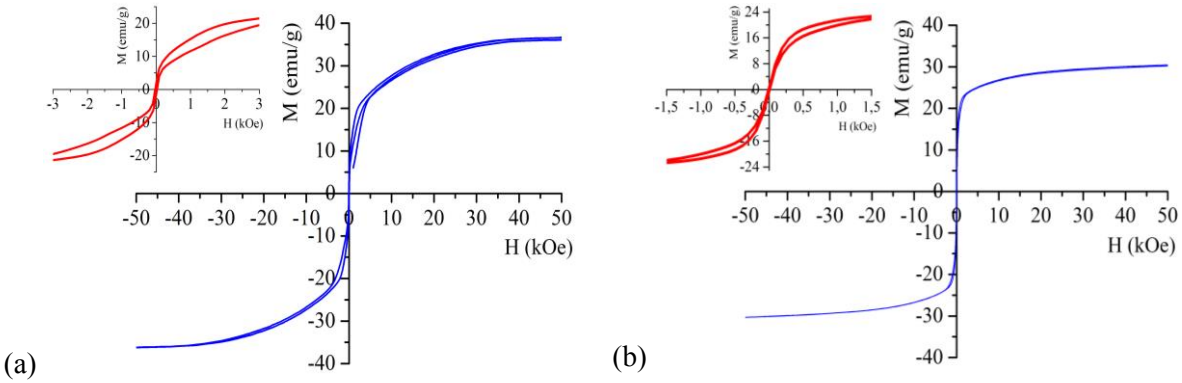

Figure 2. Hysteresis curves at 4.2 K (a) and 300 K (b) of $Ba_{0.5}Sr_{1.5}Zn_{0.5}Ni_{1.5}Fe_{11.92}Al_{0.08}O_{22}$ powder.

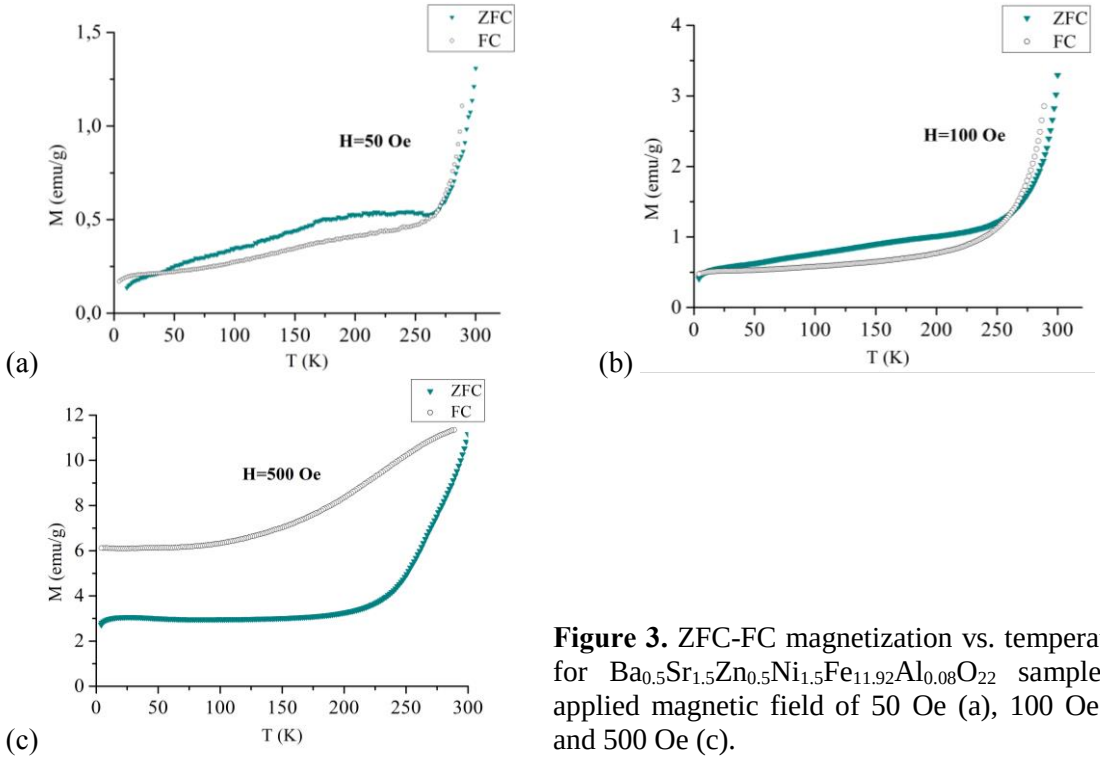

Figure 3. ZFC-FC magnetization vs. temperature for $Ba_{0.5}Sr_{1.5}Zn_{0.5}Ni_{1.5}Fe_{11.92}Al_{0.08}O_{22}$ sample at applied magnetic field of 50 Oe (a), 100 Oe (b) and 500 Oe (c).

Figure 3 shows the temperature course of the ZFC and FC magnetization curves of $Ba_{0.5}Sr_{1.5}Zn_{0.5}Ni_{1.5}Fe_{11.92}Al_{0.08}O_{22}$ polycrystalline material at magnetic fields of 50 Oe, 100 Oe, and 500 Oe in the temperature range 4.2 K – 300 K. Evidently, the external magnetic field provokes substantial spin rearrangements leading to a changed magnetic response and a corresponding shift of associated temperature points.

Figure 4 shows the temperature dependence of the ZFC and FC magnetization of $Ba_{0.5}Sr_{1.5}Zn_2Fe_{12}O_{22}$ with a single cationic substitution of either Zn or Fe, i.e., $Ba_{0.5}Sr_{1.5}Zn_{0.5}Ni_{1.5}Fe_{12}O_{22}$ and $Ba_{0.5}Sr_{1.5}Zn_2Fe_{11.92}Al_{0.08}O_{22}$.

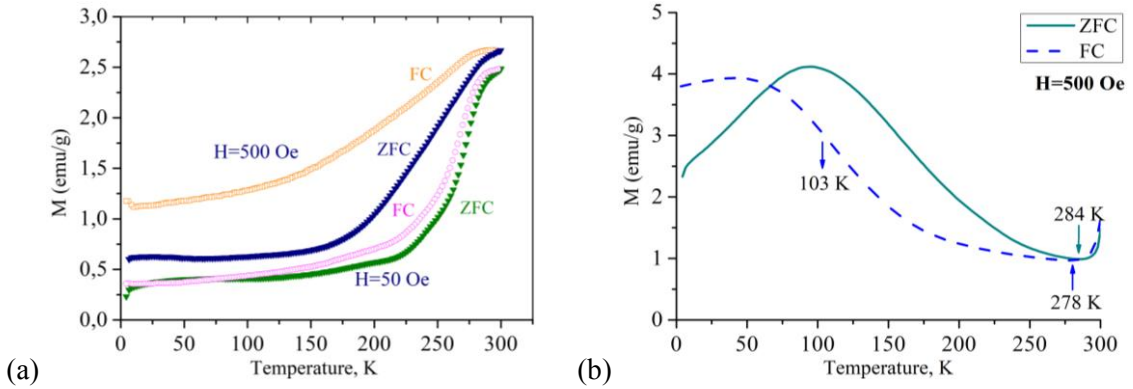

Figure 4. ZFC- and FC-magnetization vs temperature at applied magnetic field of 50 Oe and 500 Oe for $Ba_{0.5}Sr_{1.5}Zn_{0.5}Ni_{1.5}Fe_{12}O_{22}$ (a) and 500 Oe for $Ba_{0.5}Sr_{1.5}Zn_2Al_{0.08}Fe_{11.92}O_{22}$ (b) powders (under review).

As can be seen, the effect of Ni^{2+} substitution for Zn^{2+} on the behavior of magnetization is much more pronounced than that of the Fe^{3+} substitution with Al^{3+}. The magnetization increases gradually to about 250 K, and then as the temperature rises to 300 K, its increase becomes very steep. A similar behavior was observed for $Ba_{0.5}Sr_{1.5}ZnNiFe_{12}O_{22}$ [7]. By analogy with $Ba_{0.5}Sr_{1.5}ZnNiFe_{12}O_{22}$ and $Ba_{0.5}Sr_{1.5}Ni_2Fe_{12}O_{22}$, it might be inferred that a helical spin arrangement has set below 260 K for

$Ba_{0.5}Sr_{1.5}Zn_{0.5}Ni_{1.5}Fe_{11.92}Al_{0.08}O_{22}$. This temperature is higher than that of $Ba_{0.5}Sr_{1.5}Zn_{0.5}Ni_{1.5}Fe_{12}O_{22}$ without partial diamagnetic substitution of iron. Compared with $Ba_{0.5}Sr_{1.5}Zn_2Fe_{11.92}Al_{0.08}O_{22}$, no transition from a conical spin order to a spiral spin arrangement was observed in $Ba_{0.5}Sr_{1.5}Zn_{0.5}Ni_{1.5}Fe_{11.92}Al_{0.08}O_{22}$.

The behavior of ZFC-FC curves in the temperature range 260 – 300 K indicates that the magnetic order adopts the so-called intermediate phase. The transition temperature to the paramagnetic phase is much higher than room temperature, so this magnetic transition could not be observed. It can be expected that the transformation from the proper screw magnetic ordered state to the ferrimagnetic arrangement above room temperature becomes through successive metamagnetic transitions, with the evolution of the magnetic structures associated with the magnetoelectric effect according to the findings of Hiraoka et al. [11, 12] for single crystal $Ba_{0.5}Sr_{1.5}Ni_2Fe_{12}O_{22}$.

3. Conclusion

Single-phase $Ba_{0.5}Sr_{1.5}Zn_{0.5}Ni_{1.5}Fe_{11.92}Al_{0.08}O_{22}$ polycrystalline material was obtained by citric acid sol-gel auto-combustion. The partial replacement of iron with Al^{3+} leads to dilute magnetic exchange interactions and contributes to intricate changes in the magnetic response both to the temperature and an external magnetic field in comparison with the referent $Ba_{0.5}Sr_{1.5}Zn_{0.5}Ni_{1.5}Fe_{12}O_{22}$ hexaferrite. The Al^{3+} substitution raises above 260 K the temperature of the frustrated arrangement of the complex spin system toward the intermediate phase and might also increase the transition temperature of the helical spin order to the ferrimagnetic spin alignment to a higher than room temperature.

Acknowledgments

B. Georgieva was supported by the Bulgarian Ministry of Education and Science under the National Research Program “Young scientists and postdoctoral students” approved by DCM # 577/17.08.2018. This work was supported by the Bulgarian National Science Fund under contract KP-06-India-2, by a joint research project between the Bulgarian Academy of Sciences and WBI, Belgium, and by a joint research project between the Bulgarian Academy of Sciences and the Institute of Low Temperature and Structure Research, Polish Academy of Sciences.

References

[1] Pullar R 2012 *Prog. Mater. Sci*. **57** 1191–1334
[2] Kouril K, ChlanV, Štepánková H, Novák P, Knížek K, Hybler J, Kimura T, Hiraoka Y and Bursık J 2010 *J. Magn. Magn. Mater.* **322** 1243–1245
[3] Kouril K, Chlan V, Štepánková H, Telfah A, Novák P, Knížek K, Hiraoka Y and Kimura T 2010 *Acta Phys. Polonica* A **118** 732–733
[4] Hirschner J, Maryško M, Hejtmánek J, Uhrecký R, Soroka M, Buršík J, Anadón A, Aguirre M and Knížek K 2017 *Phys. Rev.* B **96** 064428
[5] Taniguchi K, Abe N, Ohtani S, Umetsu H and Arima T 2008. *Appl. Phys. Express* **1** 031301
[6] Chun S, Chai Y, Oh Y, Jaiswal-Nagar D, Haam S, Kim I, Lee B, Nam D, Ko K, Park J-H, Chung J-H and Kim K 2010 *Phys. Rev. Lett.* **104** 037204
[7] Georgieva B, Koutzarova T, Kolev S, Krezhov K, Kovacheva D, Ghelev Ch, Vertruyen B, Tran L M and Zaleski A 2019 *AIP Conf. Proc.* **2075** 010001
[8] Koutzarova T, Kolev S, Krezhov K, Georgieva B, Ghelev Ch, Kovacheva D, Vertruyen B, Closset R, Tran L M, Babij M and Zaleski A 2020 *J. Magn. Magn. Mater.* **505** 166725
[9] Raju N, Reddy S, Reddy C, Reddy P, Reddy K and Reddy V 2015 *J. Magn. Magn. Mater.* **384** 27–32
[10] El Hiti M A and Abo El Ata A M 1999 *J. Magn. Magn. Mater.* **195** 667–678
[11] Hiraoka Y, Nakamura H, Soda M, Wakabayashi Y and Kimura T 2011 *J. Appl. Phys.* **110** 033920
[12] Hiraoka Y, Tanaka Y, Kojima T, Takata Y, Oura M, Senba Y, Ohashi H, Wakabayashi Y, Shin S and Kimura T 2011 *Phys. Rev.* B **84** 064418